

# Analysis of Two Different Top-Gated simulated Graphene Nanomesh High Performance Field Effect Transistor (GNMFET)

Rohit Nimje<sup>1</sup>, Rabinder Henry<sup>2</sup>, Jayant Pawar<sup>2</sup>, Ashish Kumar Patel<sup>2</sup>, Amit Patwardhan<sup>2</sup>

<sup>1</sup>Center for Nanotechnology Research, VIT University, Vellore, Tamil Nadu, India

<sup>2</sup>Hope Foundation's, Pralhad P. Chhabria Research Center (PPCRC), Pune, Maharashtra, India.

**Abstract-** Two different types of Graphene Nanomesh Field Effect Transistor has been tested with aluminum oxide ( $Al_2O_3$ ) and Tantalum (Ta) as a gate dielectric materials. Graphene Nanomesh bandgap is engineered with Virtual NanoLab (ATK). The material parameters such as channel thickness and width of Graphene Nanomesh Filed Effect Transistor are extracted. The transistor operation is modeled with Drift-Diffusion Model Space (DDMS). The two different transistor devices are analyzed by applying various gate bias voltages. The transfer and output characteristics are observed. The functionality of the transistors are calculated for high frequency input signals. The maximum frequency is observed for aluminum oxide top-gated dielectric Graphene Nanomesh Filed Effect Transistor.

**Keywords:** Device Characterization, Device Modelling, Graphene Transistor, High Frequency

## 1. INTRODUCTION

Graphene has a unique ambipolar behavior like carrier transport phenomenon. Both electrons and holes are contribute for current conduction. Graphene Filed Effect Transistor (GFET) works for Radio Frequency (RF) applications [1].

The device performance in Radio Transmitter Units (RTU) is limited by using conventional graphene material. This is due to the bandgap limitations. The reduced gate length, carrier mobility and cut-off frequency results in short channel effects in GFET [2, 3].

This problem is being overcome in non-conventional Field Effect Transistor such as Graphene Nanomesh Field Effect Transistor (GNMFET) [3, 4]. High channel area of GFET increases channel width during alternating current (AC) operations [5, 6]. In GNMFET short channel effects are reduced due to defect (nanoholes) in graphene sheets. This is also called as Graphene Nanoribbon (GNM). Such materials can also be used for device design which can operate at high frequency.

GNMFET has many advantages. At high frequency operations conventional GFET's result in low drain current saturation. This is not the case with GNM channel and results in better saturation of the drain current. Also it has high mechanical strength and required thickness. GNMFET operates based on high mobility, and conductivity. This purely depends on a change in the gate to source voltage ( $V_{GS}$ ) at high input frequency [7, 8].

GNMFET is designed with the aluminum (Al) drain and a source electrode and gold (Au) as a top gate contact. The semiconductor device is constructed with ( $SiC/Al_2O_3/Al$ ) gate control for

GNMFET<sub>1</sub> and gate-stack ( $Si/Al_2O_3/Ta/Al_2O_3/Au$ ) technique for GNMFET<sub>2</sub> in TCAD simulator tool [9]. GNMFET developed on Silicon (Si) and Silicon Carbide (SiC) substrate are more useful for carrier transport. And also easily visible at the time of characterization [3, 10, 11, 12]. GNMFET operates on direct current (DC) gate bias voltages ( $V_{GS}$ ) which controls the drain current ( $I_D$ ). This due to high gate capacitance of  $Al_2O_3$ . The gate oxide material makes a stable difference between semiconducting nature of channel and the Aluminum (Al) electrode. This avoids drain leakage current from the device [13, 14, 8].

In Radio Transmitters units GNMFET is used for signal encoding as a frequency amplifier [13]. GNMFET has better performance at high frequency. Transistor's frequency of operation has cut-off limit called as band-stop frequency. This is very high for GNMFET with regard to conventional transistors [10, 6].

## 2. MATERIALS AND METHODS

### 2.1 Graphene bandgap opening

Graphene can be utilized for design of high-speed electronic devices, but limited by controllability of electron mobility transport in the material. GFET operates on high-speed AC signal transmission due to a short channel effect. The modeling of GNM is a new approach for nanostructure development [4]. It is possible with semi-metal material. By adding nanoholes into the graphene sheet the carrier transport phenomenon is improved in GNMFET as shown in Figure 1 [8].

The GNM is prepared using channel thickness of 5 nm. GNMFET can support higher current density than GFET. It is tuned by varying the neck width. Graphene Nanomesh developed on Virtual NanoLab. (Atomistic toolkit) [12, 4].

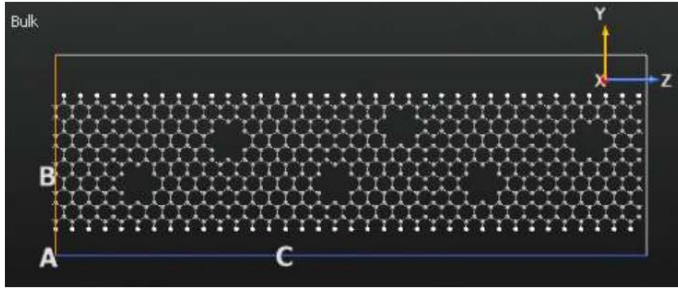


Figure.1: Graphene Nanomesh (GNM).

### 3. DESIGN METHODOLOGY

Al<sub>2</sub>O<sub>3</sub> top-gate dielectric GNMFET<sub>1</sub> structure is developed on Silicon Carbide (SiC) substrate by extracting device parameters shown in Table 1 [10, 11]. 2D structures of GNMFET have been modeled with Silvaco Atlas device

Table 1: Device Parameter for GNMFET<sub>1</sub>

Device Parameter	Region	Material
Gate Dielectric	63 nm	Al <sub>2</sub> O <sub>3</sub>
Gate-Stack	67 nm	Tantalum (Ta)
Self-Aligned Gate Dielectric Thickness (Top/Bottom)	13 nm /22 nm	Al <sub>2</sub> O <sub>3</sub> /Ta/ Al <sub>2</sub> O <sub>3</sub> /Al
Substrate	300 nm	Silicon (Si)

simulation software shown in Figure 2 [13]. The device modeling steps includes meshing, auto-grid, region identifications, material interfacing, boundary conditions material, device modeling, numerical methods and simulation with DC as well as AC input parameters. GNMFET<sub>1</sub> has been modeled on atlas design tool and separates GNM on Silicon Carbide material [14]. GNMFET<sub>1</sub> device channel is confined in gate dielectric (Al<sub>2</sub>O<sub>3</sub>) placed in between the gate contact and the GNM channel material at 22 nm range [7].

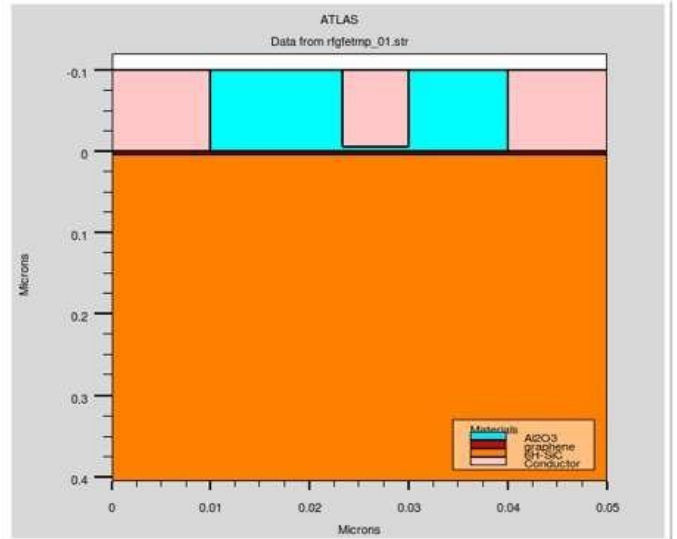


Figure 2: Device structure of GNMFET<sub>1</sub> model with Al<sub>2</sub>O<sub>3</sub> gate dielectric material extraction.

#### 3.1 Device Structure of GNMFET<sub>2</sub>

In GNMFET<sub>2</sub> structure, GNM is placed on Silicon substrate. It is confined within self-gate aligned structure called gate stacking. The material for stacking is Tantalum (Ta). The gate Gold (Au) and Tantalum (Ta) are separated by Al<sub>2</sub>O<sub>3</sub> gate dielectric material [9]. The dielectric-dielectric phenomenon of the gate stack improves the output characteristics of the GNMFET<sub>2</sub>. The carrier transported through this channel. The flow of electrons from source to drain is higher at every state with respect to the low gate voltage (V<sub>GS</sub>). Tantalum gate-stack graphene transistor [9, 13] with the same device parameter but different values of gate parameters are simulated. GNM top-gated (Al<sub>2</sub>O<sub>3</sub>) is stacked with two different metal [15]. GNMFET<sub>2</sub> structure is shown in Figure 3. The gate dielectric material parameters are listed in Table 2 [6].

Table 2: Device Parameter for GNMFET<sub>2</sub>

Device Parameter	Region	Material
Device Length	160 nm	Graphene
Metal Contacts	50 nm	Aluminum
Gate Dielectric Thickness	22 nm	Al <sub>2</sub> O <sub>3</sub>
Dielectric Width	67 nm	Al <sub>2</sub> O <sub>3</sub>

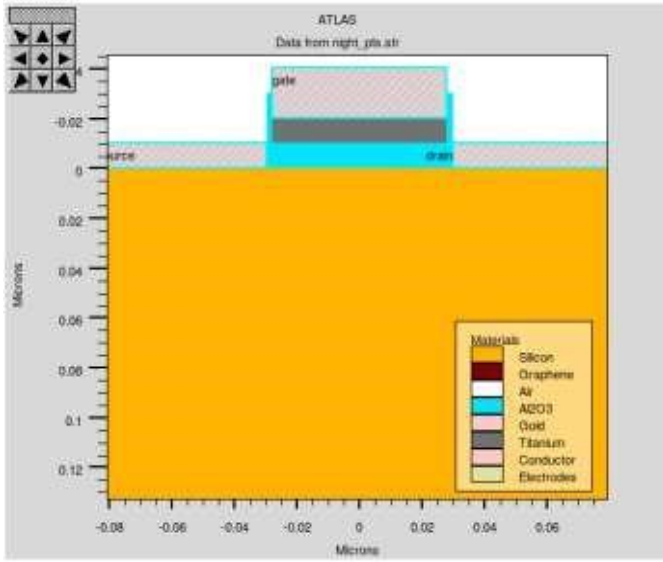


Figure 3: Device structure of self-aligned GNMFET<sub>2</sub>

In GNMFET<sub>2</sub> device gold (Au) of 50 nm thickness is deposited as a gate contact metal on the Si substrate [14]. The drain and source contact is formed by Al at 10 nm and bottom substrate of Ta at 70 nm [9]. Ohmic conduct is used to assign the electron thickness and carrier transport of the GNMFET. The top gate capacitance has been extracted using the AC analysis. This minimizes the resistance and the parasitic capacitance between source and drain during operations.

#### 4. DEVICE MODELING

##### 4.1 Drift-Diffusion Model Space (DDMS)

Both the GNMFET1 and GNMFET2 structures are modeled using Drift-Diffusion Model Space (DDMS). The operation of GNMFET is purely based on the carrier transport equations that is calculated by the DDMS device model. The utilization of DDMS is compatible with 2D semiconductor devices as compared to the Schrödinger wave equation or mode-space NEGF models. Floating body effect of GNMFET are controlled by DDMS model [6].

#### 5. RESULTS AND DISCUSSION

##### 5.1. Electric Field

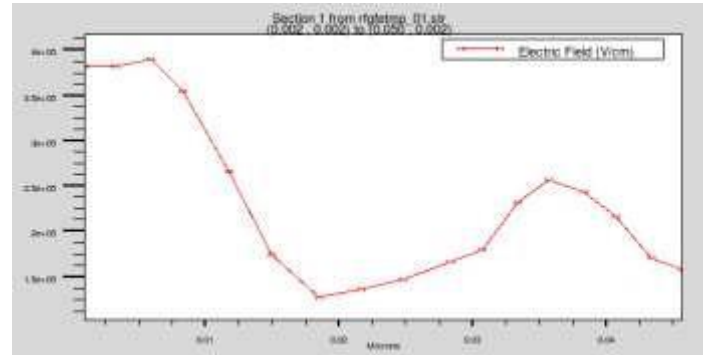


Figure 4: Electric field from source to drain in GNMFET<sub>1</sub>.

The electric field depends on the confined GNM channel material. The behavior of the electrons transmitted through GNMFET devices are recorded in the Figure 4. This representation electric field with less distortion medium and is applicable for designing high-speed electronic devices [6, 16]. Due to GNM/Al<sub>2</sub>O<sub>3</sub> interfacing, the limited electrostatic potential of Fermi energy level is equalized with zero electric fields.

##### 5.2 Total Current Density

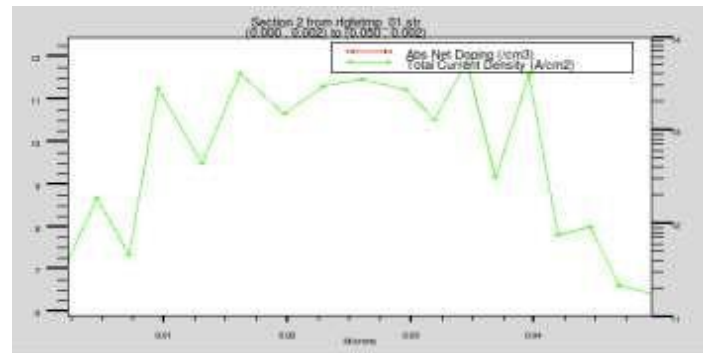
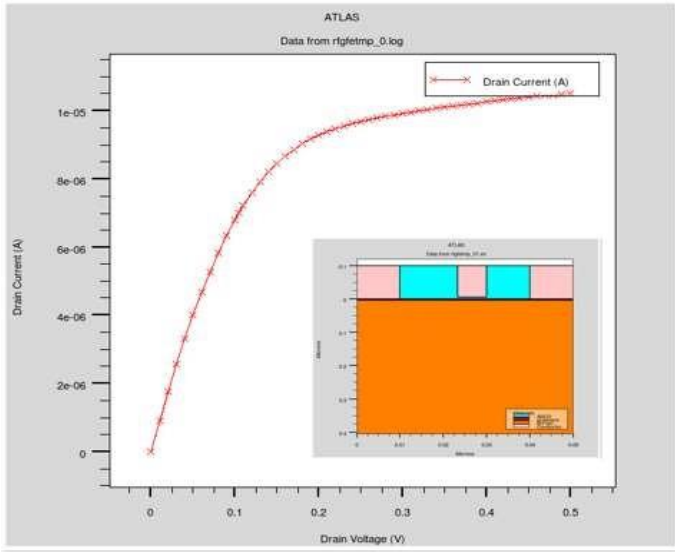


Figure 5: Total current density

Current density developed in the channel region, is due to the electrons and holes using G-R mechanism in the GNMFET devices. This is shown in Figure 5. The total carrier density is controlled by the applied gate voltage ( $V_{GS}$ ). This improves the current carrying phenomenon of the GNMFET device. Current density of the GNMFET device varies with respect to  $+V_{GS}$  and  $-V_{GS}$ , respectively.

##### 5.3 Output Characteristics



**Figure 6:**  $I_{DS}$  vs  $V_{DS}$  curve of GNMFET<sub>1</sub>

The output characteristics of the Al<sub>2</sub>O<sub>3</sub> top-gated GNMFET<sub>1</sub> is shown in Figure 6. The Al<sub>2</sub>O<sub>3</sub> gate dielectric layer is separated by GNM channel and gate (Au) contact. From source-drain, channel region is confined by drift-diffusion model space (DDMS). Effectively, curvature formation (in Figure 6) by a change in the gate to source current varies from positive to negative drain voltage ( $-0.8V_{DS}$  to  $0.6V_{DS}$ ). Gate leakage current is negligible during the measurement.

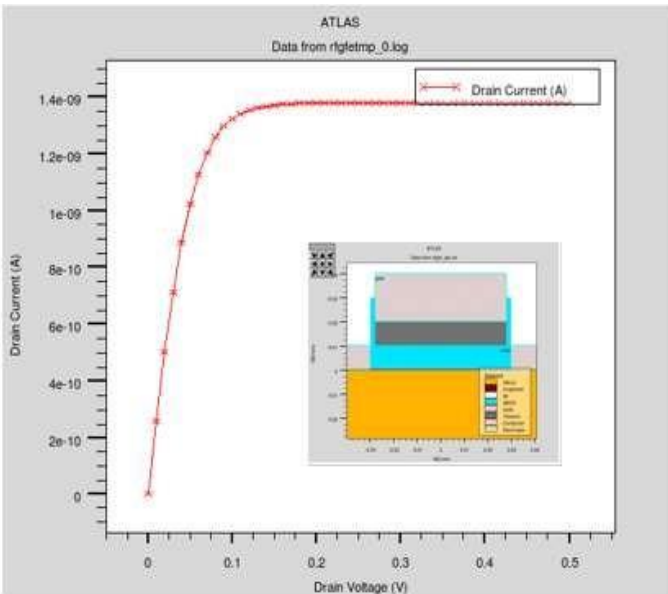


**Figure 7:**  $I_{DS}$  vs  $V_{DS}$  curve of GNMFET<sub>2</sub>

The ( $I_{DS}$  vs  $V_{DS}$ ) output characteristics are given in Figure 7. It indicates that 5 nm channel is confined within gate stack in GNMFET<sub>2</sub>. The maximum scaled ON-current is 1.73

$\text{mA}/\mu\text{m}^{-1}$  at  $-1V_{DS}$  current saturation. And this is desirable for power gain performance in high-frequency GNMFET<sub>2</sub>.

#### 5.4 Transfer Characteristics

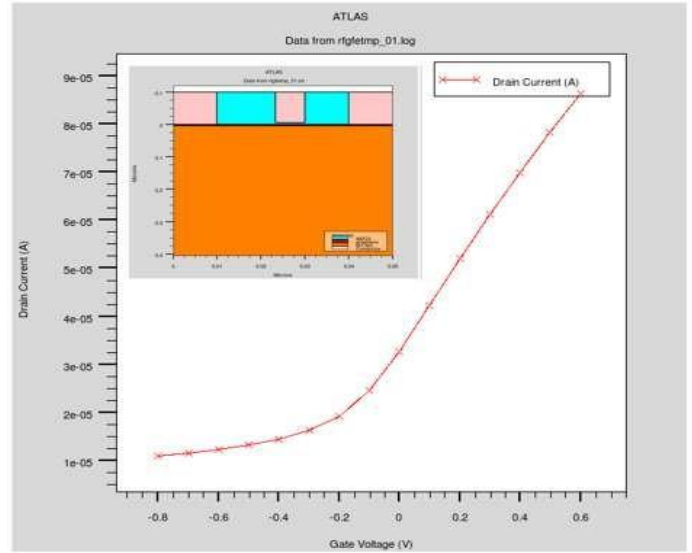


**Figure 8:**  $I_{DS}$  vs  $V_{GS}$  characteristics of GNMFET<sub>1</sub>

The GNMFET<sub>1</sub>'s transfer characteristics as inferred from the simulation results as shown in Figure 8. This describes the relationships between drain current ( $I_D$ ) gate to source voltage ( $V_{GS}$ ). The GNMFET<sub>1</sub> is considered to be switched on from low to the high with respect to applied gate voltage ( $V_{GS}$ ). The slope is high in the subthreshold region. This will always be greater than applied gate voltage ( $V_{GS} < V_{Th}$ ). This results in better switching characteristics of GNMFET<sub>1</sub>. The threshold voltage ( $V_{Th}$ ) changes while the change in  $I_D$  for a given change in  $V_{GS}$ . This is called the terminal trans-conductance ( $g_{tm}$ ) and the relationship are given in equation 1, 2 and 3 [8].

$$g_{tm} = g_{tm0} \left(1 - \frac{I_{DSS}}{|V_{GS(off)}|}\right) \quad (1)$$

Where,

$$g_{tm0} = 2 \frac{I_{DSS}}{|V_{GS(off)}|} \quad (2)$$

Therefore,

$$g_{tm} = \Delta I_D / \Delta V_{GS} \quad (3)$$

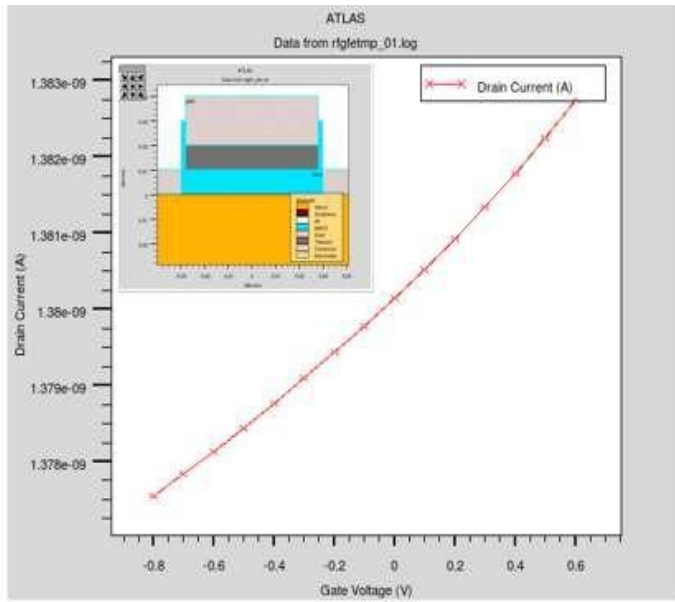


Figure 9:  $I_{DS}$  vs  $V_{GS}$  characteristics of GNMFET<sub>2</sub>

0.1V  $V_{GS}$  or less is applied to the gate dielectric material. This is for interfacing electron-hole symmetry which commonly originates from the misalignment between the work function of contact or electrodes. Hence, an increment in the negative shift Dirac point increases the drain voltage effectively. This is in line with half Dirac point change in  $V_{GS}$ . The finite element calculation top gate capacitance is 359 nF/ cm<sup>2</sup> in GNMFET<sub>2</sub> as shown in Figure 9.

### 5.5 Maximum Frequency:

From the above two transfer characteristics of the devices, GNMFET<sub>1</sub> should be more preferable to perform at high input frequency signals. GNMFET<sub>1</sub> are tested under 3 MHz input frequency. If channel length of the GNMFET<sub>1</sub> decreases, then the Dirac point is shifted towards the positive direction. This negates the short channel effects. This is also improves the strength of a signal in the transistor [5].

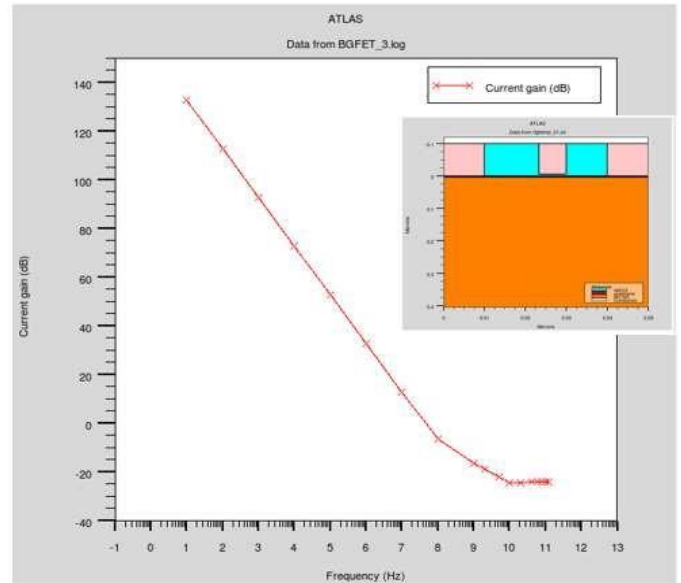


Figure 10: Maximum frequency of top-gated Al<sub>2</sub>O<sub>3</sub> dielectric GNMFET<sub>1</sub>.

The maximum frequency observed for GNMFET<sub>1</sub> is up to 10 MHz is shown in Figure 10. This produces multiple oscillations. The application of GNMFET<sub>1</sub> is for Radio transmitter Unit [5-12].

## 6. CONCLUSION

The GNMFET devices were developed by adding Drift-Diffusion Model Space (DDMS) model using Silvaco Atlas TCAD tool. Comparative analysis of both the devices showed difference in  $I_{DS}$  vs  $V_{GS}$  curve and found GNMFET<sub>1</sub> more superior than GNMFET<sub>2</sub> for high-performance in carrier transport. Output frequency of 10 MHz was achieved by GNMFET<sub>1</sub> device on giving 3 MHz input frequency. Therefore, GNMFET<sub>1</sub> can be used in Radio transmitter unit, short distance high frequency communication in military operations, satellite communication, mobile RF unit etc.

### Acknowledgement

Authors sincerely, thanks to Hope Foundation & Research Centre for the funding and support. We also thank all the team members who supported our work at Pralhad P Chhabria Research Center.

### REFERENCES

- [1] Awan, S. A., Lombardo, A., Colli, A., Privitera, G., Kulmala, T. S., Kivioja, J. M., ... & Ferrari, A. C. (2016) Transport conductivity of graphene at RF and microwave frequencies. 2D Materials, 3(1), 015010.



- [2] Schwierz, F. (2010) Graphene transistors. *Nature nanotechnology*, 5(7), 487.
- [3] Park, S., Shin, S. H., Yogeesh, M. N., Lee, A. L., Rahimi, S., & Akinwande, D. (2016) Extremely high-frequency flexible graphene thin-film transistors. *IEEE Electron Device Letters*, 37(4), 512-515.
- [4] Pasadas, F., & Jiménez, D. (2016) Large-signal model of graphene field-effect transistors—Part II: Circuit performance benchmarking. *IEEE Transactions on Electron Devices*, 63(7), 2942-2947.
- [5] Toolkit, Q. A. with Virtual NanoLab.
- [6] Silvaco Int. (2006) ATLAS User's Manual, Device Simulation Software, [www.silvaco.com](http://www.silvaco.com)
- [7] Bai, J., Zhong, X., Jiang, S., Huang, Y., & Duan, X. (2010) Graphene nanomesh. *Nature nanotechnology*, 5(3), 190.
- [8] Yu, C., He, Z. Z., Liu, Q. B., Song, X. B., Xu, P., Han, T. T., ... & Cai, S. J. (2016) Graphene amplifier MMIC on SiC substrate. *IEEE Electron Device Letters*, 37(5), 684-687.
- [9] Cheng, C., Huang, B., Liu, J., Zhang, Z., Mao, X., Xue, P., & Chen, H. (2016) A pure frequency tripler based on CVD graphene. *IEEE Electron Device Letters*, 37(6), 785-788.
- [10] Yang, X., Bonmann, M., Vorobiev, A., & Stake, J. (2016, June) Characterization of Al<sub>2</sub>O<sub>3</sub> gate dielectric for graphene electronics on flexible substrates. In *Millimeter Waves (GSMM) & ESA Workshop on Millimetre-Wave Technology and Applications, 2016 Global Symposium on* (pp. 1-4), IEEE.
- [11] Karabiyik, M., & Pala, N. (2016) Microelectronic Engineering Fabrication of Graphene Field effect Transistor with Field Controlling Electrodes to improve f<sub>T</sub>.
- [12] Nanmeni Bondja, C., Geng, Z., Granzner, R., Pezoldt, J., & Schwierz, F. (2016) Simulation of 50-nm gate graphene nanoribbon transistors. *Electronics*, 5(1), 3.
- [13] Wei, W., Pallecchi, E., Belhaj, M., Centeno, A., Amaia, Z., Vignaud, D., & Happy, H. (2016, October) Graphene field effect transistors on flexible substrate: Stable process and high RF performance. In *Microwave Integrated Circuits Conference (EuMIC), 2016 11th European* (pp. 165-168), IEEE.
- [14] Beshkova, M., Hultman, L., & Yakimova, R. (2016) Device applications of epitaxial graphene on silicon carbide. *Vacuum*, 128, 186-197.
- [15] Partida-Manzanera, T., Roberts, J. W., Bhat, T. N., Zhang, Z., Tan, H. R., Dolmanan, S. B., ... & Potter, R. J. , (2016) Comparative analysis of the effects of tantalum doping and annealing on atomic layer deposited (Ta<sub>2</sub>O<sub>5</sub>)<sub>x</sub> (Al<sub>2</sub>O<sub>3</sub>)<sub>1-x</sub> as potential gate dielectrics for GaN/Al<sub>x</sub>Ga<sub>1-x</sub>N/GaN high electron mobility transistors. *Journal of Applied Physics*, 119(2), 025303.
- [16] Wu, Y., Lin, Y. M., Bol, A. A., Jenkins, K. A., Xia, F., Farmer, D. B., ... & Avouris, P. (2011) High-frequency, scaled graphene transistors on diamond-like carbon. *Nature*, 472(7341), 74.